Contents lists available at ScienceDirect

BBA - Biomembranes

journal homepage: www.elsevier.com/locate/bbamem

Effect of tertiary amine local anesthetics on G protein-coupled receptor lateral diffusion and actin cytoskeletal reorganization

Bhagyashree D. Rao [1], Parijat Sarkar [1], Amitabha Chattopadhyay [*]

CSIR-Centre for Cellular and Molecular Biology, Uppal Road, Hyderabad 500 007, India

A B S T R A C T

Although widely used clinically, the mechanism underlying the action of local anesthetics remains elusive. Direct interaction of anesthetics with membrane proteins and modulation of membrane physical properties by anesthetics are plausible mechanisms proposed, although a combination of these two mechanisms cannot be ruled out. In this context, the role of G protein-coupled receptors (GPCRs) in local anesthetic action is a relatively new area of research. We show here that representative tertiary amine local anesthetics induce a reduction in two-dimensional diffusion coefficient of the serotonin$_{1A}$ receptor, an important neurotransmitter GPCR. The corresponding change in mobile fraction is varied, with tetracaine exhibiting the maximum reduction in mobile fraction, whereas the change in mobile fraction for other local anesthetics was not appreciable. These results are supported by quantitation of cellular F-actin, using a confocal microscopic approach previously developed by us, which showed that a pronounced increase in F-actin level was induced by tetracaine. These results provide a novel perspective on the action of local anesthetics in terms of GPCR lateral diffusion and actin cytoskeleton reorganization.

1. Introduction

Local anesthetics are a group of amphiphilic compounds, which act by blocking the transmission of nerve impulse, leading to suppression and reduction of pain in a specific part of the body. In spite of widespread clinical use of local anesthetics, the fundamental molecular mechanism behind their action remains elusive. The inherent structural as well as chemical diversity of local anesthetics makes it challenging to identify probable mechanisms of their action. Two predominant hypotheses have been proposed to explain the mechanism behind the action of local anesthetics. The protein hypothesis suggests that the specific interaction of membrane proteins with local anesthetics could modulate protein function and form the basis for anesthetic action [1–3]. On the contrary, the lipid hypothesis states that anesthesia occurs due to interaction of anesthetics with membranes that modulates membrane physical properties [4–6]. It is possible that a combination of protein and lipid-mediated effects are involved in the generation of local anesthesia since dissecting their individual contribution is not trivial

[7,8].

A common target of local anesthetics is ligand-gated ion channels [9] which belong to the family of four transmembrane domain proteins [10]. Nevertheless, the role of other membrane proteins such as G protein-coupled receptors (GPCRs) in local anesthesia has been reported [11]. GPCRs represent the largest superfamily of membrane proteins in higher eukaryotes, are hugely diverse, and are characterized by a classical seven transmembrane domain architecture [12–14]. They are major signaling hubs in cells and upon activation by a wide range of stimuli undergo concerted structural rearrangements in their transmembrane region, resulting in signal transduction to intracellular effector molecules [15,16]. GPCRs play a key role in the regulation of many vital physiological processes including metabolism, cell differentiation, neurotransmission, immune responses and pathogen entry. Due to this reason, GPCRs are potential candidates for developing new drugs [17–19] and comprise ~40% of commercially available drugs in all clinical areas [20].

GPCR function could be modulated by its dynamics which could, in

turn, regulate its interaction with membranes and act as a determinant for the efficiency of signal transduction process [21–26]. Lateral diffusion of membrane proteins and lipids controls the dynamics of protein-protein and lipid-protein interactions [27–29]. The constrained lateral diffusion of proteins and lipids has often been associated with the formation of heterogeneous composition-specific domains in membranes over a range of spatiotemporal scales [30,31]. An important source of constrained lateral diffusion in biological membranes is the intricate meshwork of actin cytoskeleton below the plasma membrane [32–34]. Actin is one of the most abundantly present cytosolic proteins in eukaryotic cells and exists in a dynamic equilibrium between monomeric (globular or G-actin) and polymeric (filamentous or F-actin) forms [35,36]. The maintenance of such dynamic equilibrium between F- and G-actin serves as a mechanism for modulating crucial downstream signal transduction pathways [37]. Previous work has shown that lateral diffusion of GPCRs is significantly affected by the actin cytoskeleton [25,38]. In this context, how local anesthetics could modulate the actin cytoskeleton and lateral diffusion of GPCRs represents an interesting question.

The serotonin$_{1A}$ receptor is an extensively studied neurotransmitter receptor in the GPCR family and facilitates multiple behavioral, neurological, and cognitive functions [39–44]. As a consequence, it has emerged as a key drug target in the development of therapeutics for diverse conditions such as neuropsychiatric disorders including anxiety and depression to even cancer [45,46]. We have previously shown that local anesthetics, including tertiary amine local anesthetics, inhibit the function of the serotonin$_{1A}$ receptor [47,48] as well as modulate the organization and dynamics of neuronal membranes [49]. To obtain further insight into the role of GPCRs in the mechanism of action of local anesthetics, in the present work, we monitored membrane dynamics of the serotonin$_{1A}$ receptor and actin cytoskeleton organization in the presence of representative tertiary amine local anesthetics (see Fig. 1) by

utilizing approaches based on confocal fluorescence microscopy. Fluorescence recovery after photobleaching (FRAP) measurements reveal that diffusion coefficient of the serotonin$_{1A}$ receptor exhibits reduction in the presence of local anesthetics, whereas mobile fraction is not affected in a major way, except in the case of tetracaine. Interestingly, actin cytoskeleton polymerization exhibits an increase in the presence of tetracaine. These results provide a new perspective to the action of local anesthetics in terms of receptor diffusion and actin organization.

2. Materials and methods

2.1. Materials

3-(4,5-Dimethylthiazol-2-yl)-2,5-diphenyl-tetrazolium bromide (MTT), dibucaine, dimethyl sulfoxide (DMSO), gentamycin sulfate, lidocaine, penicillin, poly-L-lysine, procaine, sodium bicarbonate, streptomycin, tetracaine and Triton X-100 were obtained from Sigma Chemical Co. (St. Louis, MO). Formaldehyde solution (~37–41% (w/v)) was purchased from Merck (Darmstadt, Germany). DMEM/F-12 [Dulbecco's modified Eagle's medium/nutrient mixture F-12 (Ham) (1:1)], fetal calf serum (FCS) and geneticin (G418) were from Invitrogen/Life Technologies (Grand Island, NY). Alexa Fluor 546 phalloidin was obtained from Molecular Probes/Invitrogen (Eugene, OR). All other chemicals used were of the highest available purity. Water was purified through a Millipore (Bedford, MA) Milli-Q system and used throughout.

2.2. Methods

2.2.1. Cell culture

Chinese Hamster Ovary (CHO) cells stably expressing the serotonin$_{1A}$ receptor tagged to EYFP at the C-terminus (termed as CHO-5-HT$_{1A}$R-EYFP) were maintained in DMEM/F-12 (1:1) medium supplemented
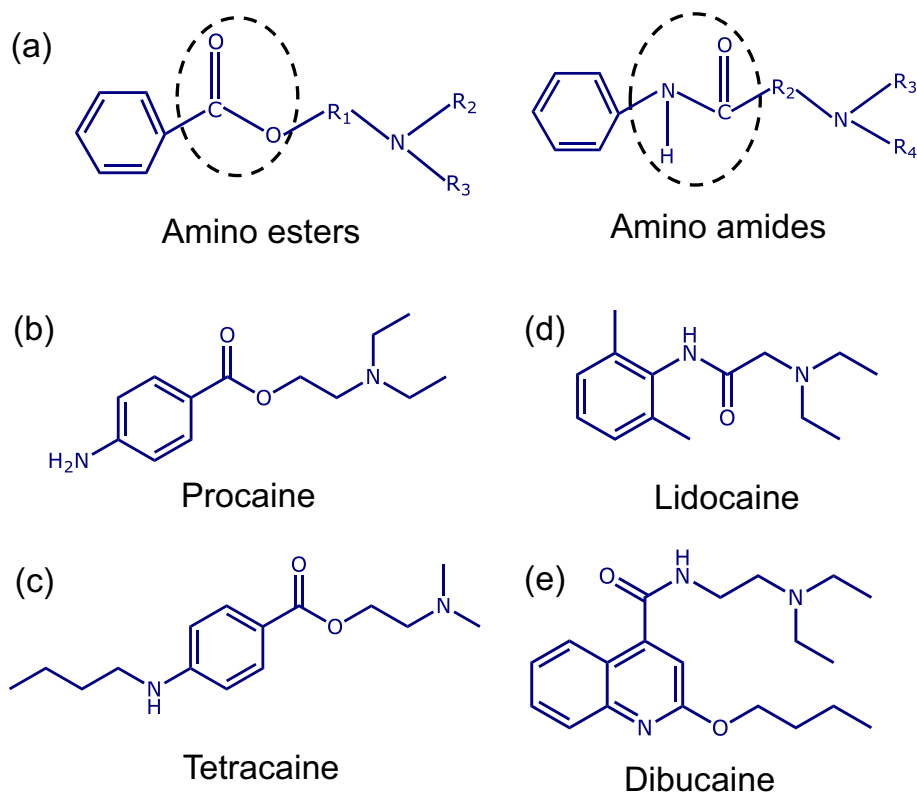

Fig. 1. Chemical structures of tertiary amine local anesthetics. (a) Chemical structures of two representative class of local anesthetics clinically used: amino esters and amino amides (the ester and amide linkages are highlighted). (b) Procaine and (c) tetracaine are representative amino ester anesthetics, whereas (d) lidocaine and (e) dibucaine are representative amino amide anesthetics. See text for other details.

with 2.4 g/l of sodium bicarbonate, 10% fetal calf serum, 60 μg/ml penicillin, 50 μg/ml streptomycin, 50 μg/ml gentamycin sulfate (complete medium), and 0.3 mg/ml G418 in a humidified atmosphere with 5% CO_2 at 37 °C.

2.2.2. Treatment of cells with local anesthetics

CHO-5-HT$_{1A}$R-EYFP cells were treated with specific concentrations of local anesthetics. Briefly, 5 mM stock solutions of local anesthetics were prepared in water and working stocks were made upon diluting the stocks in serum-free DMEM/F-12 medium. Cells were grown in complete medium for 3 days and subsequently incubated in serum-free DMEM/F-12 medium for 3 h. Cells were treated with different concentrations of the local anesthetics in serum-free DMEM/F-12 medium for 1 h at 37 °C.

2.2.3. MTT viability assay

The viability of CHO-5-HT$_{1A}$R-EYFP cells upon treatment with local anesthetics was assessed using MTT assay as described previously [50]. Briefly, ~10^4 cells were plated in poly-L-lysine coated 96-well plates and treated with a range of concentrations of the local anesthetics. Following this, cells were washed with PBS and incubated with MTT dissolved in serum-free DMEM/F-12 medium at a final concentration of 0.4 mg/ml at 37 °C for 1 h. The reduction of MTT salt by mitochondrial enzymes in live cells [51] led to formation of formazan crystals which were dissolved in DMSO and the color obtained was measured by absorbance at 540 nm in an EnSpire Multimode plate reader (Perkin Elmer, Waltham, MA).

2.2.4. FRAP measurements using confocal microscopy

Confocal imaging was carried out on an inverted Zeiss LSM 880 confocal microscope (Jena, Germany) with a Plan-Apochromat 63×/1.4 NA oil immersion objective using the 514 nm line of an argon laser [52]. Fluorescence emission was collected using the 517–606 nm bandpass with pinhole under 1 airy condition. FRAP measurements were performed at room temperature (~23 °C) on CHO-5-HT$_{1A}$R-EYFP cells treated with local anesthetics in serum-free DMEM/F-12 medium at 37 °C. The basal surface of cells that represents the plasma membrane was selected for bleaching and monitoring recovery of fluorescence, using a region of interest (ROI) of 1 μm radius. The ROI was irreversibly bleached using the highest intensity of the laser and fluorescence recovery due to diffusion into the bleached region was monitored using low-intensity of the scanning laser. Data on diffusion coefficient (D) and mobile fraction (M$_f$) were calculated from quantitative FRAP experiments where the bleached region was scanned to achieve improved temporal resolution. The bleach time point was estimated as the midpoint of the bleach duration resulting in the first post-bleach time point starting from a time t > 0. The bleaching time duration was ~215 ms and the time interval between successive scans was 200 ms. Data representing the mean fluorescence intensity in the membrane region (obtained using the Zen software (version 2.3)) within the bleached spot were corrected for background and analyzed. For a two-dimension diffusion model, FRAP data were fit to the following equation to determine the characteristic diffusion time (τ$_d$) [23]:

$$F(t) = [F(\infty) - F(0)][exp(-2\tau_d/t)(I_0(2\tau_d/t) + (I_1(2\tau_d/t))] + F(0) \qquad (1)$$

where F(t) is the mean background-corrected and normalized fluorescence intensity at time t in the membrane region within the bleached spot, F(∞) is the recovered fluorescence at time t→∞, and F(0) is the bleached fluorescence intensity at time t→0. I$_0$ and I$_1$ are modified Bessel functions. The effective two-dimensional diffusion coefficient (D) was determined from the equation [53]:

$$D = \omega^2/4\tau_d \qquad (2)$$

where ω is the radius of the bleached spot. Mobile fraction (M$_f$) was calculated according to the equation:

$$M_f = [F(\infty) - F(0)]/[F(p) - F(0)] \qquad (3)$$

where F(p) is the mean background-corrected and normalized prebleach fluorescence intensity. Non-linear curve fitting of fluorescence recovery data to Eq. (1) was carried out using the GraphPad Prism software version 4.0 (San Diego, CA).

2.2.5. F-actin labeling of cells

F-actin labeling in CHO-5-HT$_{1A}$R-EYFP cells treated with local anesthetics was performed as described previously [37]. Following treatment with anesthetics, cells were washed with PBS and fixed with ~3.5% (w/v) formaldehyde for 10 min. Fixed cells were permeabilized in PBS containing 0.5% (v/v) Triton X-100 for 6 min. Cells were then washed with PBS, stained with 0.3 μM Alexa Fluor 546 phalloidin for 60 min at room temperature, and subsequently mounted on glass slides.

2.2.6. Quantification of F-actin

F-actin cytoskeleton was imaged on an inverted Zeiss LSM 880 confocal microscope (Jena, Germany). Imaging of F-actin was performed by exciting Alexa Fluor 546 phalloidin using a 543 nm laser, and emission was collected using a bandpass of 550–650 nm. Control experiments showed that excitation of EYFP using a 543 nm laser did not result in appearance of any significant signal in the Alexa Fluor 546 channel (*i.e.*, 550–650 nm), thereby allowing clear separation of EYFP and Alexa Fluor 546 signal (data not shown). F-actin level was estimated using a quantitative high-resolution confocal microscopic technique previously developed by us [37]. Briefly, *z*-section images were acquired using a 63×/1.4 NA oil immersion objective with a fixed *z*-step size of 0.32 μm under 1 airy condition. Maximal intensity projections of 11 *z*-sections (corresponding to ~3.5 μm from the base into the cell) were obtained, and area of the projected images was calculated using the Zen software provided with the microscope. A 30% threshold intensity of the average fluorescence intensity calculated from the maximum intensity projections was used for the generation of iso-surface images. Iso-surfaces (defined as voxel contours of equal fluorescence intensity) were generated from the *z*-sections using Imaris 8.0.0 (Bitplane, Zurich, Switzerland) after thresholding the fluorescence intensity of *z*-sections, followed by application of a Gaussian filter. The estimated volumes of F-actin cytoskeleton enclosed by iso-surfaces were normalized to the projected total area of cells in a given field.

2.2.7. Statistical analysis

Significance levels were estimated using Student's two-tailed unpaired *t*-test using GraphPad Prism version 4.0 (San Diego, CA). Plots were generated using Microcal Origin version 9.7.0 (OriginLab, Northampton, MA).

3. Results

3.1. Cell viability in the presence of local anesthetics

Tertiary amine local anesthetics represent a class of commonly used local anesthetics which are characterized by an aromatic and an amine group, with an intermediate chain in between. These anesthetics could be broadly classified into two different groups, amino esters and amino amides (see Fig. 1a). The first group, commonly referred to as amino esters, is comprised of local anesthetics with an ester link between the aromatic part and the intermediate chain (shown as R$_1$ in Fig. 1a). Procaine and tetracaine belong to this group (Fig. 1b, c). The other group (amino amides) consists of local anesthetics that have an amide link between the aromatic part and the intermediate chain (R$_2$ in Fig. 1a). Lidocaine and dibucaine are members of this group (Fig. 1d, e). The ester and amide anesthetics differ in their stability and metabolism in the body [54]. Ester anesthetics are easily hydrolyzed and not very stable in solution, whereas amide anesthetics are relatively more stable. The ester

compounds are hydrolyzed by the enzyme cholinesterase in the plasma, whereas amide anesthetics are subjected to enzymatic degradation in the liver [54].

Owing to the different physicochemical properties of ester and amide anesthetics, we explored the effect of local anesthetics belonging to these two groups on lateral dynamics of a representative GPCR (i.e., the serotonin$_{1A}$ receptor) and actin cytoskeleton organization. In order to determine the concentration of anesthetics to be used for subsequent experiments, we estimated cell viability of CHO-5-HT$_{1A}$R-EYFP cells in the presence of local anesthetics spanning a range of concentrations. We used highest concentration of the individual anesthetics at which cell viability was comparable to control cells and these results are shown in Fig. 2. The concentrations of procaine, tetracaine, lidocaine and dibucaine used in subsequent studies were 1, 0.5, 2 and 0.04 mM, respectively. It is noteworthy that the concentrations of local anesthetics used in this work are within the range of clinical concentrations necessary for blocking the transmission of nerve impulse [55].

3.2. Modulation of serotonin$_{1A}$ receptor mobility monitored by FRAP measurements

Fluorescence recovery after photobleaching (FRAP) is an extensively used approach to monitor lateral diffusion of an ensemble of molecules such as lipids and proteins in biological membranes [52,56–58]. FRAP measurements involve generating a concentration gradient of fluorescent molecules by inducing irreversible photobleaching of a fraction of fluorophores in a specific area referred as the region of interest (ROI). This concentration gradient gets dissipated with time as a consequence of diffusion of fluorophores from the unbleached regions into the bleached region in the membrane. Analysis of the fluorescence recovery into the bleached region yields two important parameters, diffusion coefficient (D) and mobile fraction (M$_f$), which collectively describe receptor lateral diffusion. Diffusion coefficient is estimated from the rate at which fluorescence recovery occurs, while mobile fraction is determined from the extent of fluorescence recovery in FRAP timescale.

We have previously shown that the function of the serotonin$_{1A}$ receptor is compromised in the presence of tertiary amine local anesthetics [47]. In order to probe whether receptor mobility could be one of the factors responsible for the modulation in receptor function, we
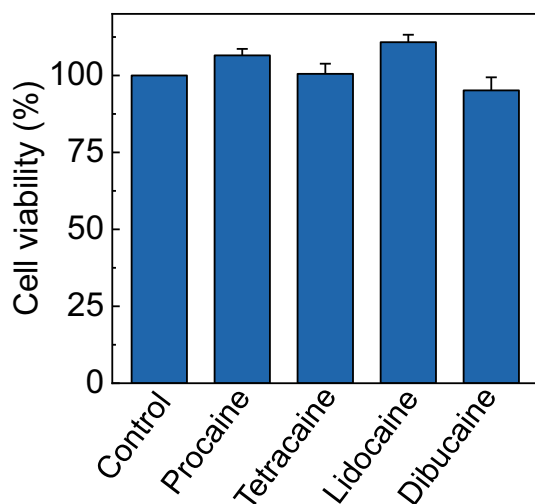
Fig. 2. MTT viability assay in the presence of local anesthetics. MTT viability assays carried out upon treatment of CHO-5-HT$_{1A}$R-EYFP cells with local anesthetics at the concentrations used in this study. The concentrations used were 1, 0.5, 2 and 0.04 mM for procaine, tetracaine, lidocaine and dibucaine, respectively. Values are expressed as percentages of viability of treated cells normalized to control cells. Data represent means ± S.E. of three independent measurements. See Materials and methods for more details.

monitored lateral diffusion of the serotonin$_{1A}$ receptor (tagged with EYFP as a reporter) utilizing FRAP measurements. Representative plots depicting the kinetics of fluorescence recovery in CHO-5-HT$_{1A}$R-EYFP cells treated with local anesthetics (along with control) are shown in Fig. 3. In all cases, the pattern of fluorescence recovery was altered upon treatment of cells with local anesthetics. We estimated the two-dimensional diffusion coefficient of the serotonin$_{1A}$ receptor using Eq. (2) and values obtained are shown in Fig. 4a and Table 1. The figure shows that the diffusion coefficient of the serotonin$_{1A}$ receptor in control cell membranes was 0.09 μm^2 s^{-1}, in agreement with our previous results [23]. As evident from the figure, diffusion coefficient exhibited a significant reduction in the presence of local anesthetics in all cases. We observed a reduction of ~30%, 47%, 39% and 37% in diffusion coefficient relative to control in presence of procaine, tetracaine, lidocaine and dibucaine, respectively (see Fig. 4a). To the best of our knowledge, these results constitute one of the first reports describing modulation of receptor lateral diffusion induced by local anesthetics. We note that the highest extent of reduction in diffusion coefficient was observed with tetracaine (also see below).

As part of FRAP measurements, we estimated the mobile fraction of serotonin$_{1A}$ receptors in the presence of local anesthetics using Eq. (3) and the values obtained are shown in Fig. 4b and Table 1. The mobile fraction is indicative of the fraction of the receptor population that is mobile in FRAP timescale and often acts as a useful indicator of constrained receptor dynamics [25]. The figure shows that the mobile fraction of the serotonin$_{1A}$ receptor in control membranes was ~82%, again in agreement with our previous results [23]. Fig. 4b shows the varying effects of local anesthetics on receptor mobile fraction. For example, whereas we observed a modest decrease in mobile fraction in presence of lidocaine (~8%) and dibucaine (~16%), the mobile fraction of the receptor remained essentially unchanged in presence of procaine. In contrast, the mobile fraction change was maximum (~57%) in case of tetracaine. When viewed along with the change in diffusion coefficient (see above), it appears that tetracaine was able to induce a drastic dynamic change in the receptor environment.

3.3. Effect of local anesthetics on organization of actin cytoskeleton

The above results clearly bring out environmental changes experienced by the serotonin$_{1A}$ receptor in the presence of local anesthetics, thereby modulating receptor lateral dynamics, particularly in the case of tetracaine. Although FRAP is an excellent tool for providing a 'dynamic window' for measuring receptor dynamics (lateral diffusion), a limitation of FRAP measurements is that it lacks the information to identify the molecular players responsible for such changes in receptor dynamics. We therefore chose to examine this further and explored organizational changes at the actin cytoskeleton level which is known to control receptor dynamics [25,33].

From a dynamic perspective, cellular signaling could be viewed as a consequence of the differential mobility characteristics of interacting components in membranes. Lateral diffusion of membrane lipids and proteins can undergo modulation upon perturbation of cytoskeletal proteins. The meshwork of actin cytoskeleton is coupled to the plasma membrane and facilitates the formation of heterogeneous membrane domains which results in confined diffusion of membrane components and could trigger diverse signaling responses [59,60]. In this context, lateral diffusion of receptors in membranes could be a major determinant of the efficiency of signal transduction processes [61]. We have previously shown that actin cytoskeleton dependent dynamics of the serotonin$_{1A}$ receptor exhibits close correlation with intracellular signaling by the receptor [25].

In order to assess whether altered dynamics of the serotonin$_{1A}$ receptor could be due to actin cytoskeleton reorganization induced by local anesthetics, we quantified F-actin by a confocal fluorescence microscopy based approach previously developed by us [37]. For this, we treated CHO-5-HT$_{1A}$R-EYFP cells with local anesthetics, followed by F-
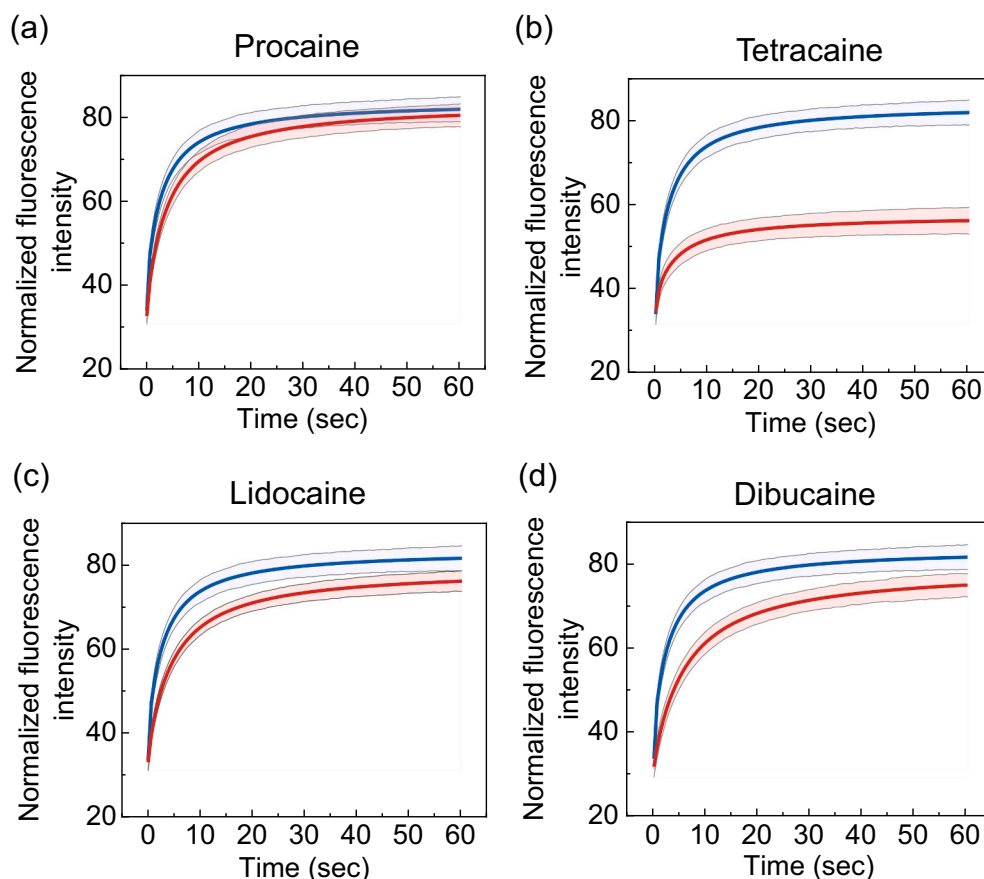
Fig. 3. Fluorescence recovery from FRAP measurements. Representative fluorescence recovery curves showing the rate of recovery in CHO-5-HT$_{1A}$R-EYFP cells treated with the corresponding local anesthetics (red): (a) procaine, (b) tetracaine, (c) lidocaine and (d) dibucaine, along with control condition (blue) in all cases. The curves shown are non-linear regression fits of the experimental data obtained using Eq. (1). Shaded areas represent the regions encompassed by error bars from individual data points in all plots. The concentrations of the local anesthetics were the same as in Fig. 2. Data represent means ± S.E. from at least four independent experiments. See Materials and methods for other details. (For interpretation of the references to color in this figure legend, the reader is referred to the web version of this article.)

actin labeling with phalloidin and quantification of F-actin. The organization of the actin cytoskeleton in presence of local anesthetics is shown in Fig. 5 (left panel). The figure shows confocal images of the actin cytoskeleton (labeled with Alexa Fluor 546 phalloidin) of cells treated with local anesthetics. Iso-surface images corresponding to the projected images are shown in Fig. 5 (right panel). In order to estimate F-actin in a quantitative manner, the volumes enclosed by the iso-surfaces were normalized to the projected area of cells in each case. Fig. 6 shows the content of F-actin upon treatment with local anesthetics quantitated this way. The figure shows that the effect of local anesthetics on actin cytoskeleton organization was negligible in all cases (as apparent from F-actin levels), except in the case of tetracaine. Interestingly, treatment with tetracaine resulted in a significant increase (~20%) in F-actin level relative to control cells, possibly due to enhanced F-actin polymerization under this condition. We attribute the large reduction in the mobile fraction of the serotonin$_{1A}$ receptor in the presence of tetracaine (Fig. 4b) to considerable reorganization in the actin cytoskeletal network.

4. Discussion

The role of GPCRs in local anesthetic action is an emerging area of research motivated by the fact that the mechanism underlying the action of local anesthetics is still not well understood [62], even after more than a century of its discovery [63]. As mentioned above, direct effects (*via* specific interaction with membrane proteins) [1–3] or indirect effects (*via* modulation of bulk membrane physical properties) [4–6,64] have been implicated in anesthetic action. Yet another mechanism for anesthetic action could be a combination of direct and indirect effects. In this work, we show that tertiary amine local anesthetics reduce the two-dimensional diffusion coefficient of the serotonin$_{1A}$ receptor in CHO-K1

cells. The effect of local anesthetics on the mobile fraction of the receptor is more interesting. Tetracaine showed the maximum reduction in the receptor mobile fraction, whereas other local anesthetics exhibited either modest change or no significant change. Taken together, we conclude that tetracaine is unique in its ability to induce maximum change in receptor dynamics. These results are reinforced by confocal microscopic quantitation of F-actin content since tetracaine resulted in the most pronounced increase in F-actin level.

Tetracaine has earlier been shown to induce distinct structural changes in brain spectrin [65] and destabilize phase-separated membranes, resulting in membrane fluidization in model membranes [66]. In addition, tetracaine has been shown to induce membrane interdigitation, curvature changes and solubilization of membranes [67,68], and reduce line tension at the boundary of liquid ordered/liquid disordered domains in ternary model membranes [69]. In a previous study, tetracaine was found to affect the integrity of mitochondrial membranes [70]. Importantly, tetracaine has been shown to possess stronger anesthetic action in comparison with other tertiary amine local anesthetics [70].

Our results show that tetracaine leads to dynamic reorganization of the actin cytoskeleton, as apparent from a pronounced increase in F-actin level (Fig. 6) which could play a major role in constrained dynamics of the serotonin$_{1A}$ receptor (Fig. 4). A close look at earlier literature revealed that there are reports describing the ability of tetracaine to perturb cellular cytoskeleton. For example, tetracaine was reported to alter cell morphology and induce reorganization of the actin cytoskeleton [71], although no quantitative information was provided due to lack of an assay that could quantitate actin. Differential effect of local anesthetics on receptor mobility in fibroblasts and lymphocytes was also hypothesized to be a consequence of the action of anesthetics on membrane-associated microtubules and microfilaments [72].
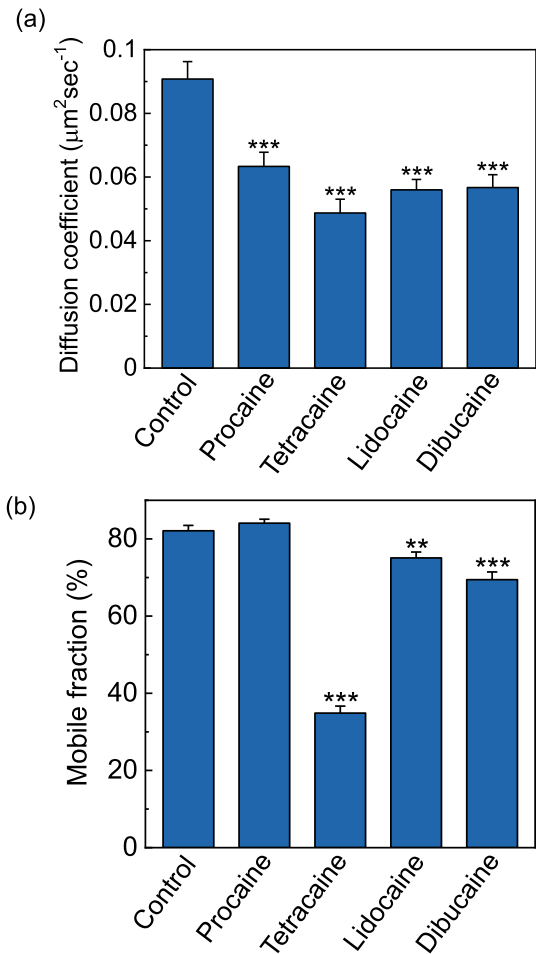
(a)

(b)

Fig. 4. Receptor mobility parameters in presence of local anesthetics. (a) Diffusion coefficient (D) of the serotonin$_{1A}$ receptor in CHO-5-HT$_{1A}$R-EYFP cells in presence of various local anesthetics estimated using Eq. (2). Modulation in D value (means ± S.E.) averaged over ~50 independent measurements from at least four experiments (*** corresponds to significant ($p < 0.001$) difference in D in the presence of local anesthetics relative to control cells). (b) Mobile fraction (M$_f$) of the receptor upon treatment with the local anesthetics calculated using Eq. (3). Modulation in M$_f$ value (means ± S.E.) averaged over ~50 independent measurements from at least four experiments (** corresponds to significant ($p < 0.01$) difference in M$_f$ in case of lidocaine, whereas *** corresponds to significant ($p < 0.001$) difference in M$_f$ in presence of tetracaine and dibucaine, relative to control condition). See Materials and methods for other details.

Table 1

Diffusion coefficients (D) and mobile fractions (M$_f$) of serotonin$_{1A}$ receptors in presence of tertiary amine local anesthetics.

Experimental condition	D ($\mu m^2 s^{-1}$) mean ± S.E.	M$_f$ (%) mean ± S.E.	N[a]
Control	0.091 (±0.006)	82.1 (±1.4)	47
Procaine	0.063 (±0.004)	84.1 (±1.0)	47
Tetracaine	0.049 (±0.004)	34.9 (±1.8)	48
Lidocaine	0.056 (±0.003)	75.1 (±1.5)	70
Dibucaine	0.057 (±0.004)	69.4 (±2.0)	58

[a] N represents the number of independent measurements. See Materials and methods for other details.

Lateral diffusion of membrane proteins and its modulation play an important role in cellular signaling [21,22,25,73]. In this context, by utilizing FRAP analysis of the serotonin$_{1A}$ receptor, we previously showed that destabilization of the actin cytoskeleton results in an
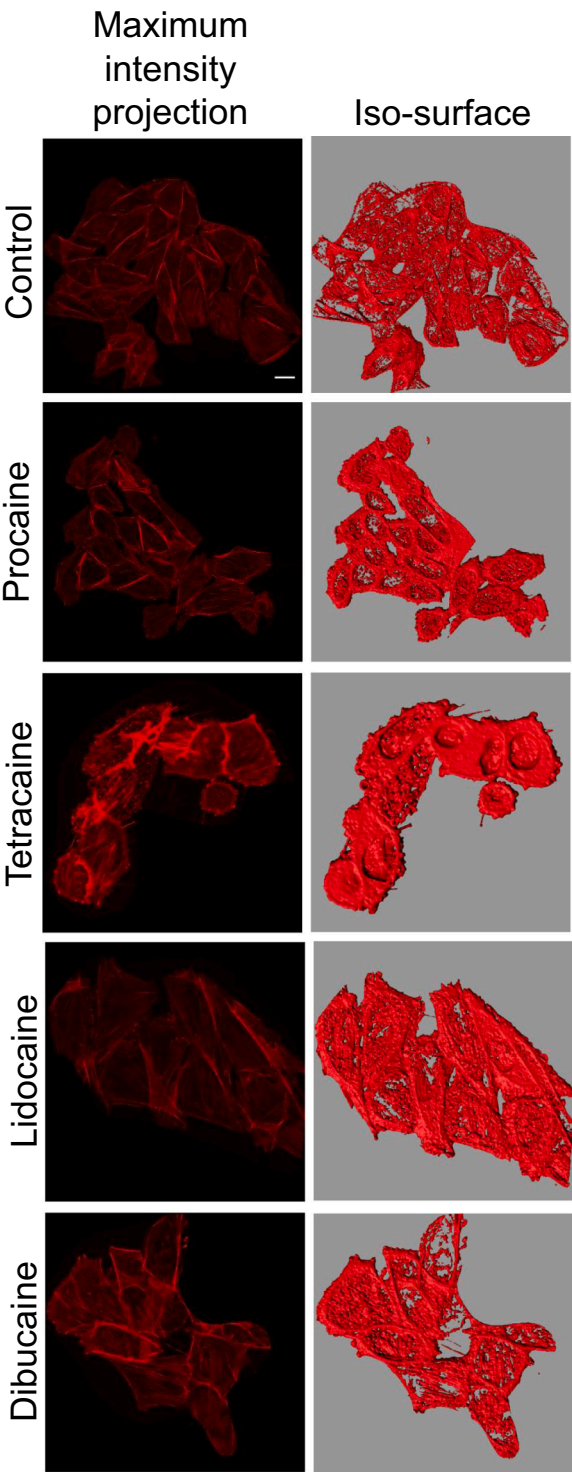
Maximum intensity projection   Iso-surface

Fig. 5. Change in the actin cytoskeleton upon treatment with local anesthetics. Organization of actin cytoskeleton in CHO-5-HT$_{1A}$R-EYFP cells treated with specific concentration of tertiary amine local anesthetics. The concentrations of the local anesthetics were the same as in Fig. 2. The actin cytoskeleton was labeled with Alexa Fluor 546 phalloidin. The figure shows projections of 11 sections from the base of the coverslip (~3.5 μm from the base into the cell). Representative projected images (maximum intensity projection) for control cells and cells treated with local anesthetics are shown in the left panel. The scale bar represents 10 μm. Iso-surface of the sections corresponding to the maximum intensity projections were generated using the iso-surface tool in Imaris. The respective iso-surface for control cells and cells treated with local anesthetics are shown in the right panel. See Materials and methods for other details.
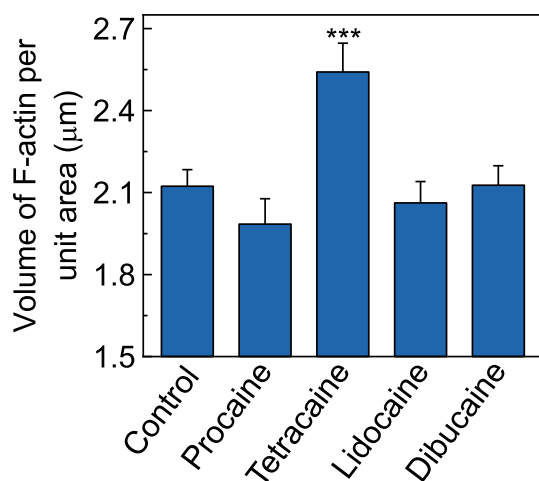
Fig. 6. Quantitation of F-actin upon treatment with local anesthetics. In order to quantitate F-actin, the volume enclosed by the iso-surface (Fig. 5) was normalized to the projected area (from Fig. 5) of cells using the built-in Zen software (version 2.3) program in LSM 880 confocal microscope. Values obtained upon quantitation of F-actin in control and CHO-5-HT$_{1A}$R-EYFP cells treated with anesthetics are shown. Data represent means ± S.E. of at least ~60 independent measurements from four experiments (*** corresponds to significant ($p < 0.001$) difference in F-actin content in cells treated with tetracaine relative to control cells). See Materials and methods for other details.

increase in mobile fraction of the receptor [25]. Interestingly, the increase in mobile fraction exhibited a tight correlation with the efficiency in ligand-mediated signaling, suggesting that signaling by the serotonin$_{1A}$ receptor is regulated by the actin cytoskeleton, possibly by the regulation of receptor mobility. In a recent work, we measured lateral diffusion of the serotonin$_{1A}$ receptor using single particle tracking (SPT) under control and actin-destabilized conditions [73]. Our analysis showed that actin destabilization led to alteration in receptor diffusion, which is manifested as an increase in functional readouts (ligand binding and cAMP signaling) of the receptor. In a recent elegant work, high plasticity in GPCR dynamics was shown to be important for receptor trafficking and regulation of receptor activity [26]. A temperature-dependent correlation between mobile fraction of a GPCR and signal transduction has also been previously reported [74]. In another work, lateral diffusion of a GPCR has been shown to be modulated upon cholesterol depletion which resulted in increased fluidity of the hydrophobic membrane region and impaired G-protein coupling [75]. We conclude that receptor dynamics and its interplay with the actin cytoskeleton could emerge as relevant factors in the mechanism of action of local anesthetics.

Declaration of competing interest

The authors declare that they have no known competing financial interests or personal relationships that could have appeared to influence the work reported in this paper.

Acknowledgments

References

[1] H.R. Arias, Role of local anesthetics on both cholinergic and serotonergic ionotropic receptors, Neurosci. Biobehav. Rev. 23 (1999) 817–843.
[2] N.P. Franks, W.R. Lieb, Seeing the light. Protein theories of general anesthesia, Anesthesiology 101 (2004) 235–237.
[3] J.F. Butterworth, G.R. Strichartz, Molecular mechanisms of local anesthesia: a review, Anesthesiology 72 (1990) 711–734.
[4] D. Papahadjopoulos, Studies on the mechanism of action of local anesthetics with phospholipid model membranes, Biochim. Biophys. Acta 265 (1972) 169–186.
[5] B. Rehberg, B.W. Urban, D.S. Duch, The membrane lipid cholesterol modulates anesthetic actions on a human brain ion channel, Anesthesiology 82 (1995) 749–758.
[6] M.A. Pavel, E.N. Petersen, H. Wang, R.A. Lerner, S.B. Hansen, Studies on the mechanism of general anesthesia, Proc. Natl. Acad. Sci. U. S. A. 117 (2020) 13757–13766.
[7] E. de-Paula, S. Schreier, Molecular and physicochemical aspects of local anesthetic-membrane interaction, Braz. J. Med. Biol. Res. 29 (1996) 877–894.
[8] P. Lirk, M.W. Hollmann, G. Strichartz, The science of local anesthesia: basic research, clinical application, and future directions, Anesth. Analg. 126 (2018) 1381–1392.
[9] L. Coyne, G. Lees, Ligand gated ion channels: crucial targets for anaesthetics? Curr. Anaesth. Critic. Care 13 (2002) 334–342.
[10] M.O. Ortells, G.G. Lunt, Evolutionary history of the ligand-gated ion channel superfamily of receptors, Trends Neurosci. 18 (1995) 121–127.
[11] K. Minami, Y. Uezono, Gq protein-coupled receptors as targets for anesthetics, Curr. Pharm. Des. 12 (2006) 1931–1937.
[12] D.M. Rosenbaum, S.G.F. Rasmussen, B.K. Kobilka, The structure and function of G-protein-coupled receptors, Nature 459 (2009) 356–363.
[13] V. Katritch, V. Cherezov, R.C. Stevens, Structure-function of the G protein-coupled receptor superfamily, Annu. Rev. Pharmacol. Toxicol. 53 (2013) 531–556.
[14] A. Chattopadhyay, GPCRs: lipid-dependent membrane receptors that act as drug targets, Adv. Biol. 2014 (2014) 143023.
[15] W.I. Weis, B.K. Kobilka, The molecular basis of G protein-coupled receptor activation, Annu. Rev. Biochem. 87 (2018) 897–919.
[16] S.C. Erlandson, C. McMahon, A.C. Kruse, Structural basis for G protein-coupled receptor signaling, Annu. Rev. Biophys. 47 (2018) 9.1–9.18.
[17] K.A. Jacobson, New paradigms in GPCR drug discovery, Biochem. Pharmacol. 98 (2015) 541–555.
[18] R.M. Cooke, A.J.H. Brown, F.H. Marshall, J.S. Mason, Structures of G protein-coupled receptors reveal new opportunities for drug discovery, Drug Discov. Today 20 (2015) 1355–1364.
[19] A.S. Hauser, M.M. Attwood, M. Rask-Andersen, H.B. Schiöth, D.E. Gloriam, Trends in GPCR drug discovery: new agents, targets and indications, Nat. Rev. Drug Discov. 16 (2017) 829–842.
[20] K. Sriram, P.A. Insel, G protein-coupled receptors as targets for approved drugs: how many targets and how many drugs? Mol. Pharmacol. 93 (2018) 251–258.
[21] D.A. Jans, R. Peters, P. Jans, F. Fahrenholz, Vasopressin V₂-receptor mobile fraction and ligand-dependent adenylate cyclase activity are directly correlated in LLC-PK₁ renal epithelial cells, J. Cell Biol. 114 (1991) 53–60.
[22] P.D. Calvert, V.I. Govardovskii, N. Krasnoperova, R.E. Anderson, J. Lem, C. L. Makino, Membrane protein diffusion sets the speed of rod phototransduction, Nature 411 (2001) 90–94.
[23] T.J. Pucadyil, S. Kalipatnapu, K.G. Harikumar, N. Rangaraj, S.S. Karnik, A. Chattopadhyay, G-protein-dependent cell surface dynamics of the human serotonin₁ₐ receptor tagged to yellow fluorescent protein, Biochemistry 43 (2004) 15852–15862.
[24] T.J. Pucadyil, A. Chattopadhyay, The human serotonin₁ₐ receptor exhibits G-protein-dependent cell surface dynamics, Glycoconj. J. 24 (2007) 25–31.
[25] S. Ganguly, T.J. Pucadyil, A. Chattopadhyay, Actin cytoskeleton-dependent dynamics of the human serotonin₁ₐ receptor correlates with receptor signaling, Biophys. J. 95 (2008) 451–463.
[26] L. Veya, J. Piguet, H. Vogel, Single molecule imaging deciphers the relation between mobility and signaling of a prototypical G protein-coupled receptor in living cells, J. Biol. Chem. 290 (2015) 27723–27735.
[27] P.G. Saffman, M. Delbrück, Brownian motion in biological membranes, Proc. Natl. Acad. Sci. U. S. A. 72 (1975) 3111–3113.
[28] P.F.F. Almeida, W.L.C. Vaz, Lateral diffusion in membranes, in: R. Lipowsky, E. Sackmann (Eds.), Handbook of Biological Physics, Elsevier, 1995, pp. 305–357.
[29] M. Edidin, Getting there is only half the fun, Curr. Top. Membr. 43 (1996) 1–13.
[30] K. Jacobson, O.G. Mouritsen, R.G.W. Anderson, Lipid rafts: at a crossroad between cell biology and physics, Nat. Cell Biol. 9 (2007) 7–14.
[31] E. Sezgin, I. Levental, S. Mayor, C. Eggeling, The mystery of membrane organization: composition, regulation and roles of lipid rafts, Nat. Rev. Mol. Cell Biol. 18 (2017) 361–374.
[32] J. Kwik, S. Boyle, M. Edidin, Membrane cholesterol, lateral mobility, and the phosphatidylinositol 4,5-bisphosphate-dependent organization of cell actin, Proc. Natl. Acad. Sci. U. S. A. 100 (2003) 13964–13969.
[33] A. Kusumi, C. Nakada, K. Ritchie, K. Murase, K. Suzuki, H. Murakoshi, R.S. Kasai, J. Kondo, T. Fujiwara, Paradigm shift of the plasma membrane concept from the two-dimensional continuum fluid to the partitioned fluid: high-speed single-molecule tracking of membrane molecules, Annu. Rev. Biophys. Biomol. Struct. 34 (2005) 351–378.
[34] A. Kusumi, T.K. Fujiwara, R. Chadda, M. Xie, T.A. Tsunoyama, Z. Kalay, R.S. Kasai, K.G.N. Suzuki, Dynamic organizing principles of the plasma membrane that

regulate signal transduction: commemorating the fortieth anniversary of Singer and Nicolson's fluid-mosaic model, Annu. Rev. Cell Dev. Biol. 28 (2012) 215–250.

[35] T.D. Pollard, Actin and actin-binding proteins, Cold Spring Harb. Perspect. Biol. 8 (2016) a018226.

[36] A.J. Davidson, W. Wood, Unravelling the actin cytoskeleton: a new competitive edge? Trends Cell Biol. 26 (2016) 569–576.

[37] S. Ganguly, R. Saxena, A. Chattopadhyay, Reorganization of the actin cytoskeleton upon G-protein coupled receptor signaling, Biochim. Biophys. Acta 1808 (2011) 1921–1929.

[38] D. Calebiro, F. Rieken, J. Wagner, T. Sungkaworn, U. Zabel, A. Borzi, E. Cocucci, A. Zürn, M.J. Lohse, Single-molecule analysis of fluorescently labeled G-protein-coupled receptors reveals complexes with distinct dynamics and organization, Proc. Natl. Acad. Sci. U. S. A. 110 (2013) 743–748.

[39] T.J. Pucadyil, S. Kalipatnapu, A. Chattopadhyay, The serotonin$_{1A}$ receptor: a representative member of the serotonin receptor family, Cell. Mol. Neurobiol. 25 (2005) 553–580.

[40] S. Kalipatnapu, A. Chattopadhyay, Membrane organization and function of the serotonin$_{1A}$ receptor, Cell. Mol. Neurobiol. 27 (2007) 1097–1116.

[41] C.P. Müller, R.J. Carey, J.P. Huston, M.A. De Souza Silva, Serotonin and psychostimulant addiction: focus on 5-HT$_{1A}$-receptors, Prog. Neurobiol. 81 (2007) 133–178.

[42] J.A. Gordon, R. Hen, The serotonergic system and anxiety, NeuroMolecular Med. 5 (2004) 27–40.

[43] Y. Glikmann-Johnston, M.M. Saling, D.C. Reutens, J.C. Stout, Hippocampal 5-HT$_{1A}$ receptor and spatial learning and memory, Front. Pharmacol. 6 (2015) 289.

[44] P. Sarkar, S. Mozumder, A. Bej, S. Mukherjee, J. Sengupta, A. Chattopadhyay, Structure, dynamics and lipid interactions of serotonin receptors: excitements and challenges, Biophys. Rev. (2020), https://doi.org/10.1007/s12551-020-00772-8.

[45] E. Lacivita, M. Leopoldo, F. Berardi, R. Perrone, Serotonin 5-HT$_{1A}$ receptor, an old target for new therapeutic agents, Curr. Top. Med. Chem. 8 (2008) 1024–1034.

[46] F. Fiorino, B. Severino, E. Magli, A. Ciano, G. Caliendo, V. Santagada, F. Frecentese, E. Perissutti, 5-HT$_{1A}$ receptor: an old target as a new attractive tool in drug discovery from central nervous system to cancer, J. Med. Chem. 57 (2014) 4407–4426.

[47] S. Kalipatnapu, A. Chattopadhyay, Interaction of serotonin$_{1A}$ receptors from bovine hippocampus with tertiary amine local anesthetics, Cell. Mol. Neurobiol. 24 (2004) 403–422.

[48] B.D. Rao, S. Shrivastava, A. Chattopadhyay, Effect of local anesthetics on serotonin$_{1A}$ receptor function, Chem. Phys. Lipids 201 (2016) 41–49.

[49] B.D. Rao, S. Shrivastava, S. Pal, A. Chattopadhyay, Effect of local anesthetics on the organization and dynamics of hippocampal membranes: a fluorescence approach, J. Phys. Chem. B 123 (2019) 639–647.

[50] G. Viswanathan, M. Jafurulla, G.A. Kumar, T.R. Raghunand, Dissecting the membrane cholesterol requirement for mycobacterial entry into host cells, Chem. Phys. Lipids 189 (2015) 19–27.

[51] D.T. Vistica, P. Skehan, D. Scudiero, A. Monks, A. Pittman, M.R. Boyd, Tetrazolium-based assays for cellular viability: a critical examination of selected parameters affecting formazan production, Cancer Res. 51 (1991) 2515–2520.

[52] P. Sarkar, A. Chattopadhyay, Exploring membrane lipid and protein diffusion by FRAP, in: R. Prasad, A. Singh (Eds.), Analysis of Membrane Lipids, Springer, 2020, pp. 119–141.

[53] D.E. Koppel, M.P. Sheetz, M. Schindler, Lateral diffusion in biological membranes. A normal-mode analysis of diffusion on a spherical surface, Biophys. J. 30 (1980) 187–192.

[54] B.G. Covino, Pharmacology of local anesthetic agents, Br. J. Anaesth. 58 (1986) 701–716.

[55] Z. Xiong, C. Bukusoglu, G.R. Strichartz, Local anesthetics inhibit the G protein-mediated modulation of K$^+$ and Ca^{2+} currents in anterior pituitary cells, Mol. Pharmacol. 55 (1999) 150–158.

[56] M. Edidin, Fluorescence photobleaching and recovery, FPR, in the analysis of membrane structure and dynamics, in: S. Damjanovich, M. Edidin, J. Szöllõsi, L. Trón (Eds.), Mobility and Proximity in Biological Membranes, CRC, Boca Raton, FL, 1994, pp. 109–135.

[57] J. Lippincott-Schwartz, E. Snapp, A. Kenworthy, Studying protein dynamics in living cells, Nat. Rev. Mol. Cell Biol. 2 (2001) 444–456.

[58] A. Chattopadhyay, M. Jafurulla, Novel insights in membrane biology utilizing fluorescence recovery after photobleaching, Adv. Exp. Med. Biol. 842 (2015) 27–40.

[59] K.F. Meiri, Membrane/cytoskeleton communication, Subcell. Biochem. 37 (2004) 247–282.

[60] J.N. Byrum, W. Rodgers, Membrane-cytoskeleton interactions in cholesterol-dependent domain formation, Essays Biochem. 57 (2015) 177–187.

[61] P.A. Liebman, A historical perspective on the lateral diffusion model of GTPase activation and related coupling of membrane signaling proteins, Cell. Logist. 4 (2014), e29389.

[62] K. Minami, Y. Uezono, The recent progress in research on effects of anesthetics and analgesics on G protein-coupled receptors, J. Anesth. 27 (2013) 284–292.

[63] P.J. Watson, The mode of action of local anaesthetics, J. Pharm. Pharmacol. 12 (1960) 257–292.

[64] H. Tsuchiya, M. Mizogami, Interaction of local anesthetics with biomembranes consisting of phospholipids and cholesterol: mechanistic and clinical implications for anesthetic and cardiotoxic effects, Anesthesiol. Res. Pract. 2013 (2013) 297141.

[65] A. Chakrabarti, M. Patra, Differential interactions of two local anesthetics with phospholipid membrane and nonerythroid spectrin: localization in presence of cholesterol and ganglioside, GM$_1$, Biochim. Biophys. Acta 1848 (2015) 821–832.

[66] K. Sugahara, N. Shimokawa, M. Takagi, Destabilization of phase-separated structures in local anesthetic-containing model biomembranes, Chem. Lett. 44 (2015) 1604–1606.

[67] S. Kaneshina, H. Matsuki, T. Hata, H. Okuno, M. Kusube, N. Tamai, Local anesthetic tetracaine induces the interdigitation of lipid bilayers, Int. Congr. Ser. 1283 (2005) 320–321.

[68] S. Hu, T. Zao, H. Li, D. Cheng, Z. Sun, Effect of tetracaine on dynamic reorganization of lipid membranes, Biochim. Biophys. Acta 1862 (2020), 183351.

[69] K. Sugahara, N. Shimokawa, M. Takagi, Thermal stability of phase-separated domains in multicomponent lipid membranes with local anesthetics, Membranes 7 (2017) 33.

[70] C. Tarba, C. Crăcium, A comparative study of the effects of procaine, lidocaine, tetracaine and dibucaine on the functions and ultrastructure of isolated rat liver mitochondria, Biochim. Biophys. Acta 1019 (1990) 19–28.

[71] G.L. Nicholson, J.R. Smith, G. Poste, Effects of local anesthetics on cell morphology and membrane-associated cytoskeletal organization in BALB/3T3 cells, J. Cell Biol. 68 (1976) 395–402.

[72] G. Poste, D. Papahadjopoulos, G.L. Nicholson, Local anesthetics affect transmembrane cytoskeletal control of mobility and distribution of cell surface receptors, Proc. Natl. Acad. Sci. U. S. A. 72 (1975) 4430–4434.

[73] S. Shrivastava, P. Sarkar, P. Preira, L. Salomé, A. Chattopadhyay, Role of actin cytoskeleton in dynamics and function of the serotonin$_{1A}$ receptor, Biophys. J. 118 (2020) 944–956.

[74] D.A. Jans, I. Pavo, A mechanistic role for polypeptide hormone receptor lateral mobility in signal transduction, Amino Acids 9 (1995) 93–109.

[75] J. Brejchová, J. Sýkora, P. Ostašov, L. Merta, L. Roubalová, J. Janáček, M. Hof, P. Svoboda, TRH-receptor mobility and function in intact and cholesterol-depleted plasma membrane of HEK293 cells stably expressing TRH-R-eGFP, Biochim. Biophys. Acta 1848 (2015) 781–796.